



Open Archive TOULOUSE Archive Ouverte (OATAO)

OATAO is an open access repository that collects the work of Toulouse researchers and makes it freely available over the web where possible.

This is an author-deposited version published in : <http://oatao.univ-toulouse.fr/>
Eprints ID : 4722

To link to this article : DOI : 10.1007/s11664-010-1274-5
URL : <http://dx.doi.org/10.1007/s11664-010-1274-5>

To cite this version : Chamoire, A. and Gascoin, F. and Estournès, Claude and Caillat, T. and Tédenac, J.-C. (2010) *High-Temperature Transport Properties of Yb_{4-x}Sm_xSb₃*. Journal of Electronic Materials, vol. 39 (n° 9). pp. 1579-1582. ISSN 0361-5235

Any correspondance concerning this service should be sent to the repository administrator: staff-oatao@inp-toulouse.fr.

High-Temperature Transport Properties of $\text{Yb}_{4-x}\text{Sm}_x\text{Sb}_3$

A. CHAMOIRE,^{1,4,6} F. GASCOIN,^{1,5} C. ESTOURNÈS,² T. CAILLAT,³ and J.-C. TÉDENAC¹

1.—Institut Charles Gerhardt Montpellier, Equipe PMOF, UMR 5253 CNRS-ENSCM-UM2-UM1, Université Montpellier II, 34095 Montpellier, France. 2.—CIRIMAT, PNF2 MHT, Université Paul Sabatier, 33062 Toulouse, France. 3.—Jet Propulsion Laboratory, California Institute of Technology, Pasadena, CA 91109, USA. 4.—*Present address:* Department of Mechanical Engineering, The OSU, Columbus, OH 43210, USA. 5.—ENSICAEN CNRS, UMR 6508, Lab CRISMAT, 14050, Caen 4, France. 6.—e-mail: achamoire@gmail.com; odraix@hotmail.com

Polycrystalline L_4Sb_3 ($\text{L} = \text{La, Ce, Sm, and Yb}$) and $\text{Yb}_{4-x}\text{Sm}_x\text{Sb}_3$, which crystallizes in the anti- Th_3P_4 structure type ($I-43d$ no. 220), were synthesized via high-temperature reaction. Structural and chemical characterization were performed by x-ray diffraction and electronic microscopy with energy-dispersive x-ray analysis. Pucks were densified by spark plasma sintering. Transport property measurements showed that these compounds are *n*-type with low Seebeck coefficients, except for Yb_4Sb_3 , which shows semimetallic behavior with hole conduction above 523 K. By partially substituting Yb by a trivalent rare earth we successfully improved the thermoelectric figure of merit of Yb_4Sb_3 up to 0.7 at 1273 K.

Key words: Yb_4Sb_3 , anti- Th_3P_4 , spark plasma sintering, thermoelectrics

INTRODUCTION

Thermoelectric performance is estimated by the dimensionless figure of merit $ZT = \alpha^2 T / (\rho \kappa)$, where α is the Seebeck coefficient ($\mu\text{V/K}$), ρ is the electrical resistivity ($\text{m}\Omega \text{ cm}$), and κ is the sum of the electronic part and the lattice part of the thermal conductivity (mW/cm K).

Therefore, good thermoelectric materials must combine high Seebeck coefficients with low electrical resistivities and thermal conductivities. However, these three contributions are connected via the carrier concentration, so that improving one usually degrades the others, thus limiting the ZT enhancement.

Rare-earth chalcogenides with Th_3P_4 -type structure have been systematically studied by Gschneidner et al.¹ and Wood.² Indeed, the chemical formulae of such compounds can be written as $\text{R}_{3-x}\text{V}_x\text{X}_4$ ($\text{R} = \text{lanthanides}$, $\text{X} = \text{S, Se, Te}$), where x represents the rare-earth vacancy (V), which is limited to $0 < x < 1/3$. For $x = 1/3$ there are no charge carriers

available for conduction, making the system insulating. By decreasing the number of vacancies, free electrons are introduced, and rare-earth chalcogenides become *n*-type conductors. Thus the charge carrier concentration can be tuned easily, and several compositions of such solid solutions show good *n*-type properties for thermoelectric applications. One of the best is a member of the $\text{La}_{3-x}\text{Te}_4$ solid solution, exhibiting $ZT > 1$ at high temperature.^{3–5} Rare-earth pnictogenides have been less well investigated for thermoelectric applications. While they do not form solid solutions, the structure is very complex and has great flexibility with regard to interstitials, which can integrate heavy elements. Additionally, anionic and cationic sites can be partially substituted. All these features can reduce the lattice thermal conductivity or allow fine tuning of the charge carrier concentration and consequently enhanced ZT .

Most of the L_4Sb_3 compounds ($\text{L} = \text{lanthanides}$) crystallize in the anti- Th_3P_4 structure type, first reported by Hohnke and Parthé.⁶ In this structural arrangement, the Sb anions in 12a Wyckoff position are 8-coordinated by two interpenetrating Yb tetrahedra forming a *bis*-disphenoid (Fig. 1). The Yb

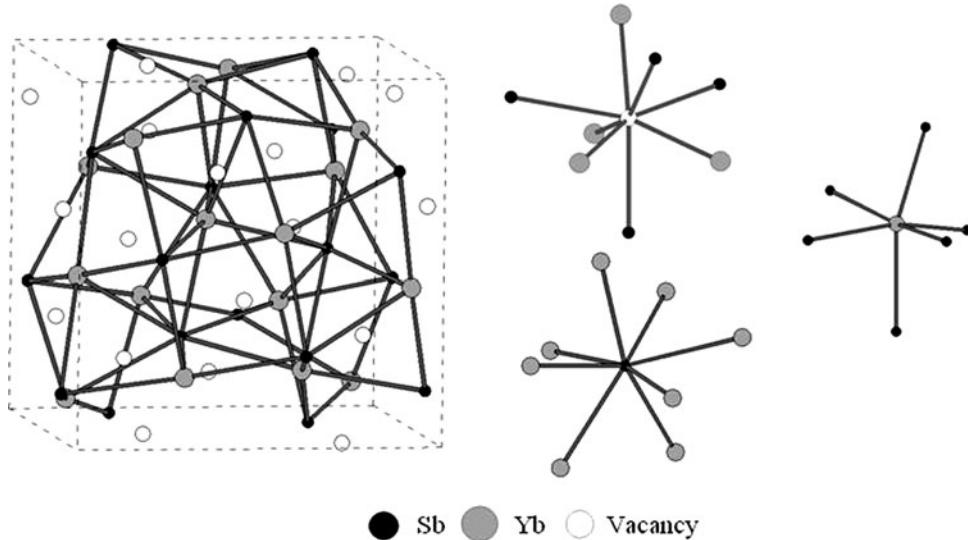


Fig. 1. Cubic crystal structure of Yb_4Sb_3 and coordination environments of individual atoms.

cations in 16c position lie at the center of a distorted Sb octahedron, and vacant sites in 12b position are coordinated by two interpenetrating Sb and Yb tetrahedra, thus forming a distorted square antiprism.

This work focuses on the transport properties of L_4Sb_3 ($\text{L} = \text{La, Ce, Sm, and Yb}$) and substitutions that can be made on the cationic site of Yb_4Sb_3 to improve thermoelectric properties.

EXPERIMENTAL PROCEDURES

L_4Sb_3 ($\text{L} = \text{La, Ce, Yb, and Sm}$) and $\text{Yb}_{4-x}\text{Sm}_x\text{Sb}_3$ were prepared by high-temperature synthesis. Stoichiometric amounts of the pure elements were directly loaded into a niobium container inside a glove box. This container was arc-welded shut under argon and in turn enclosed in a fused-silica tube under secondary vacuum (2×10^{-6} mbar to 5×10^{-6} mbar). The ampoule was heated to 1323 K, followed by a quench and subsequent anneal between 1073 K and 1173 K. Crystallographic analysis was carried out using x-ray diffraction (XRD) (Philips X'Pert) and structure refinement by Rietveld method using the program Fullprof.⁷ Composition and microstructure were checked by electronic microscopy with energy-dispersive x-ray spectroscopy. Polycrystalline samples were densified by spark plasma sintering (SPS) using a Dr Sinter 2080 SPS device following a 35 min cycle under uniaxial pressure of 50 MPa up to 1573 K. Magnetic susceptibility was measured from 2 K to 300 K, using a superconducting quantum interference device (SQUID) magnetometer from Quantum Design. Electrical resistivity (ρ),⁸ Seebeck coefficient (α),⁹ and thermal conductivity (κ)¹⁰ were measured as a function of temperature (from 300 K to 1273 K) on at least 90% dense pucks.

RESULTS AND DISCUSSION

Binaries L_4Sb_3

The synthesized binary compounds La_4Sb_3 , Ce_4Sb_3 , Sm_4Sb_3 , and Yb_4Sb_3 crystallize in the anti- Th_3P_4 structure (Fig. 2) with $a = 9.65 \text{ \AA}$, 9.51 \AA , 9.31 \AA , and 9.32 \AA ($\pm 0.005 \text{ \AA}$), respectively, in good agreement with previous works.^{11–14} Aging studies on the four compounds showed that these materials are stable in air, but a few signs of amorphization are observed on XRD analysis after 5 months. They are also stable at high temperature under inert atmosphere up to 1573 K.

Measurements were performed to at least 1100 K, with the exception of La_4Sb_3 . The 300 K Seebeck coefficients are in good agreement with those reported by Bucher et al.¹⁵ for La_4Sb_3 , Sm_4Sb_3 , and Yb_4Sb_3 . All the binaries except Yb_4Sb_3 showed *n*-type behavior from room temperature up to 1273 K (Fig. 3a and b). The Seebeck coefficients were small and negative, and did not exhibit strong temperature dependence, especially Sm_4Sb_3 , which displays a quasiconstant coefficient. However, the α of Yb_4Sb_3 (Fig. 3b) increased linearly with temperature and suggests a transition from *n*- to *p*-type conduction at 523 K that indicates a semimetallic character. It reached $70 \mu\text{V/K}$ at 1273 K, much higher than that of a metal. Electrical resistivity (Fig. 3b) also increased linearly with temperature from about 0.22 at 300 K to $1.25 \text{ m}\Omega \text{ cm}$ at 1273 K. So, the transport property data of Yb_4Sb_3 and those of the most “metallic” materials from the solid solution $\text{La}_3\text{Te}_4\text{-La}_2\text{Te}_3$ ³ (La_3Te_4) are of approximately the same magnitude at high temperature. This similarity suggests that the transport properties of Yb_4Sb_3 can be improved by tuning the carrier concentration.

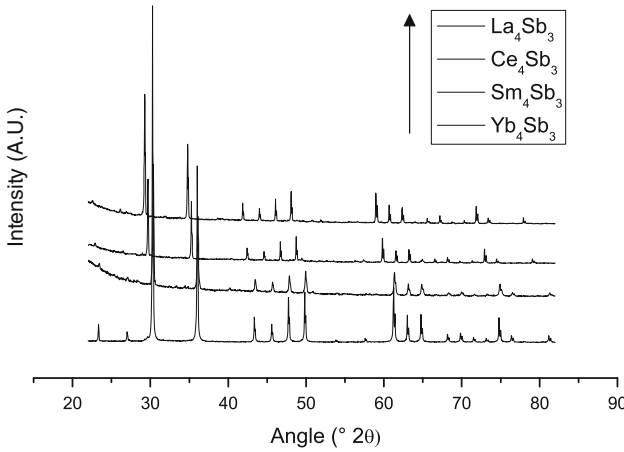


Fig. 2. XRD patterns of L_4Sb_3 , $L = \text{La}, \text{Ce}, \text{Sm}$, and Yb .

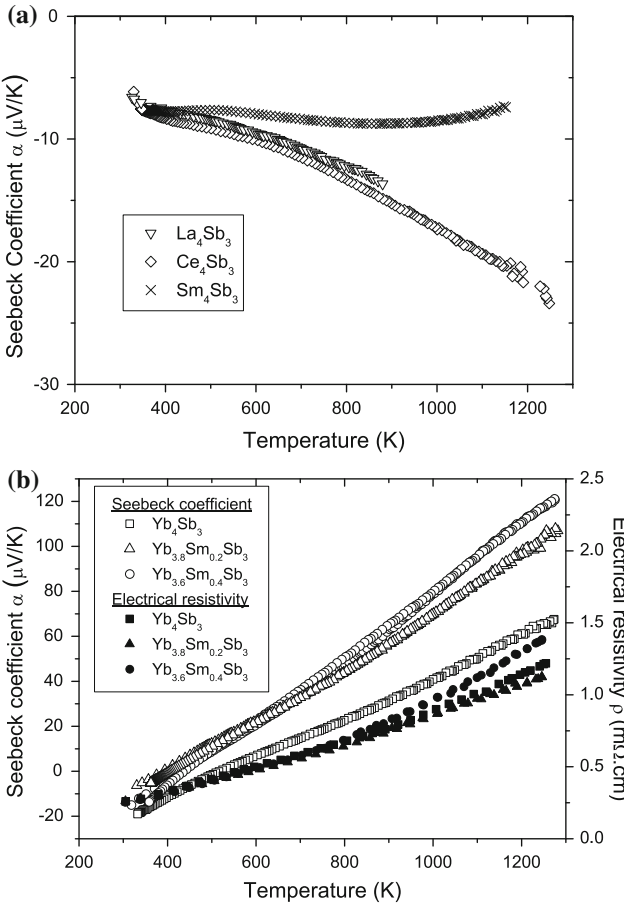


Fig. 3. (a) Seebeck coefficient of L_4Sb_3 ($L = \text{La, Ce, Sm}$) and (b) Seebeck coefficient and resistivity of Yb_4Sb_3 and $\text{Yb}_{4-x}\text{Sm}_x\text{Sb}_3$ ($x = 0.2, 0.4$) versus temperature.

The temperature dependence of the molar magnetic susceptibility ($\chi = M/H$, normalized per Yb) is in reasonable agreement with previous work¹⁶ (Fig. 4) but is much flatter. Yb_4Sb_3 shows a typical valence fluctuating behavior with a broad peak at 240 K. By fitting the low-temperature data with a

modified Curie–Weiss law we find that Yb_4Sb_3 is mainly divalent and contains less than 1% Yb^{3+} . This is low compared with previous measurements made on single crystals (average of 34%¹⁷). This could be due to the presence of a small amount of oxides such as Yb_2O_3 or other magnetic impurities undetectable via XRD.

If we consider the Zintl formalism, we can estimate that Yb_4Sb_3 is electron deficient with more than 3.8 holes per unit cell. Therefore, substitution of Yb by a trivalent or tetravalent rare earth should reduce the electron carrier density, thus improving the transport properties.

Solid Solution: $\text{Yb}_{4-x}\text{Sm}_x\text{Sb}_3$

We substituted Sm for Yb up to $x = 0.5$ to 0.6 without changing the crystal structure. The unit cell parameter, refined using the Rietveld method, is plotted versus Sm content in Fig. 4a. We see, as expected, that the lattice constant increases linearly with Sm content, from 9.32 Å to 9.38 Å (± 0.005 Å) for $\text{Yb}_{3.4}\text{Sm}_{0.6}\text{Sb}_3$. However the substitution proves not to be energetically favorable at higher x . Pure

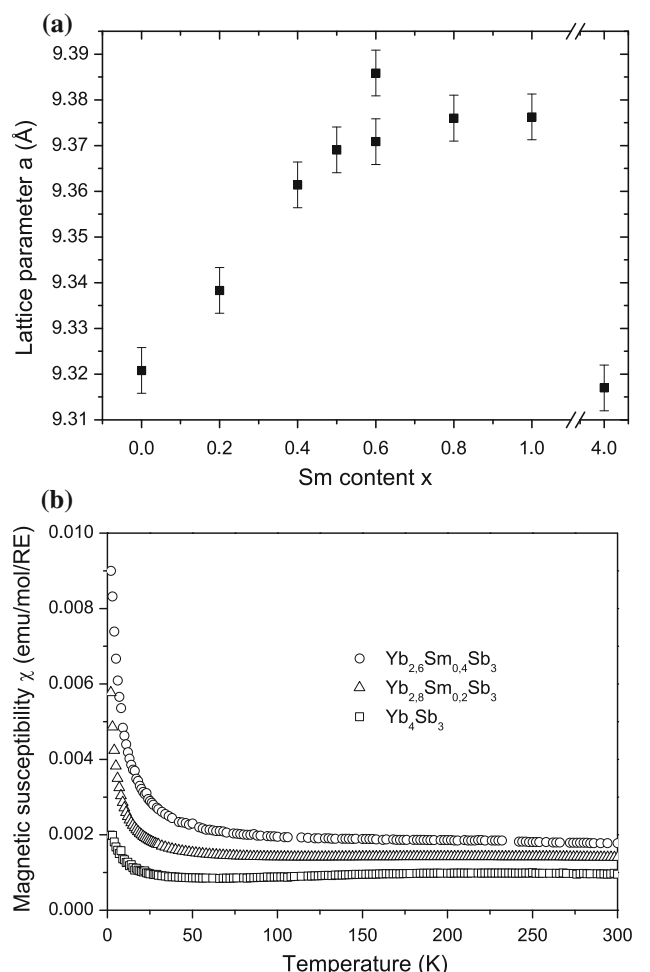


Fig. 4. $\text{Yb}_{4-x}\text{Sm}_x\text{Sb}_3$: (a) cell parameter evolution versus Sm content(x) and (b) molar magnetic susceptibility versus temperature.

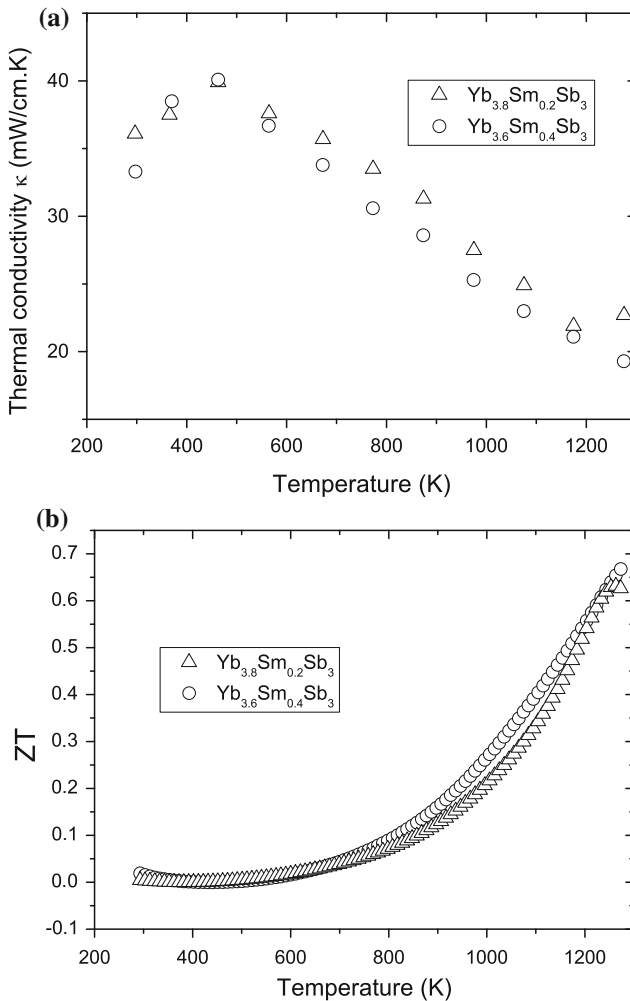


Fig. 5. (a) Thermal conductivity and (b) figure of merit ZT of $\text{Yb}_{4-x}\text{Sm}_x\text{Sb}_3$ ($x = 0.2, 0.4$) versus temperature.

samples are difficult to obtain even with long annealing times. After reaching these limits, a rock-salt-type solid solution $\text{Sm}_{1-x}\text{Yb}_x\text{Sb}$ begins to form.

The magnetic behavior (Fig. 4b) is not greatly affected by the substitutions; we observe a small increase of magnetic susceptibility as a function of Sm content, indicating a slight increase of magnetic rare earth in the system (Sm^{3+} or Yb^{3+}).

The transport properties were measured for $\text{Yb}_{4-x}\text{Sm}_x\text{Sb}_3$ ($x = 0.2, 0.4$) as a function of temperature and are compared with those of the initial binary in Fig. 3b. The Seebeck coefficient was still linear and increased with Sm content until reaching $120 \mu\text{V/K}$ at 1273 K for $\text{Yb}_{3.6}\text{Sm}_{0.4}\text{Sb}_3$, which is almost twice that of Yb_4Sb_3 . These results could indicate that the charge carrier concentration was decreased by the substitution, in good agreement

with the increase of the quantity of magnetic rare earth in the system. The electrical resistivity is not as strongly affected by the substitutions, reaching $1.4 \text{ m}\Omega \text{ cm}$ at 1273 K for $x = 0.4$.

The thermal conductivity (Fig. 5a) showed a maximum for all compositions of the solid solution around 473 K, where it reached 40 mW/cm K , and then decreased linearly with increasing temperature. We finally obtained a ZT of almost 0.7 at 1273 K for both substituted compounds (Fig. 5b).

CONCLUSIONS

Transport property measurements taken on L_4Sb_3 ($\text{L} = \text{La}, \text{Ce}, \text{Sm}$, and Yb) show that most of these compounds are n -type with low Seebeck coefficients except for Yb_4Sb_3 , which shows a transition from n - to p -type at 523 K with typical semimetallic behavior.

We show that substitution of Yb by Sm improves the Seebeck coefficient by lowering the carrier concentration. Work to further increase the thermopower of such phases is underway. These investigations will cover other type of substitutions as well as the possibility of partially filling interstitial sites.

REFERENCES

1. K.A. Gschneidner Jr., J.F. Nakahara, B.J. Beaudry, and T. Takeshita, *Mater. Res. Soc. Symp. Proc.* 97, 359 (1987).
2. C. Wood, *Rep. Prog. Phys.* 51, 459 (1988).
3. L.R. Danielson, M.N. Alexander, C. Vining, R.A. Lockwood, and C. Wood, *Seventh International Conference on Thermoelectric Energy Conversion* (Arlington, TX, 16–18 March 1988), p. 71.
4. A. May, J. Snyder, and J.-P. Fleurial, *Space Technology and Applications International Forum* (Albuquerque, NM, 10–14 February 2008), ed. M.S. El-Genk, American Institute of Physics, Melville, NY, p. 672.
5. A. May, J.-P. Fleurial, and J. Snyder, *Phys. Rev. B* 78, 125205 (2008).
6. D. Hohnke and E. Parthé, *Acta Cryst.* 21, 435 (1966).
7. J. Rodriguez-Carvajal, *Physica B* 192, 55 (1993).
8. L.J. Van der Pauw, *Philips Res. Rep.* 13, 1 (1958).
9. C. Wood, D. Zoltan, and G. Stapfer, *Rev. Sci. Instrum.* 56, 5 (1985).
10. W.J. Parker, R.J. Jenkins, C.P. Butler, and G.L. Abbott, *J. Appl. Phys.* 32, 1679 (1961).
11. R.J. Gambino, *J. Less-Common Met.* 12, 344 (1967).
12. R.E. Bodnar and H. Steinfink, *Inorg. Chem.* 6, 327 (1967).
13. Y. Wang, L.D. Calvert, and J.B. Taylor, *Acta Cryst.* B36, 221 (1980).
14. A. Ochiai, S. Nakai, A. Oyamada, T. Suzuki, and T. Kasuya, *J. Magn. Magn. Mater.* 47–48, 570 (1985).
15. E. Bucher, A.S. Cooper, D. Jaccard, and J. Sierra, *Valence Instabilities and Related Narrow Band Phenomena*, ed. R.D. Parks (New York: Plenum, 1977), p. 529.
16. A. Ochiai, T. Suzuki, and T. Kasuya, *J. Phys. Soc. Jpn.* 59, 4129 (1990).
17. S. Suga, S. Ogawa, H. Namatame, M. Tanigushi, A. Kakizaki, T. Ishii, A. Fujimori, S. Oh, H. Kato, T. Miyahara, A. Ochiai, T. Suzuki, and T. Kasuya, *J. Phys. Soc. Jpn.* 58, 4534 (1989).